

A more accurate numerical max-convolution method for sub-quadratic Bayesian inference with additive factors

Julianus Pfeuffer
Eberhard-Karls-Universität Tübingen

Oliver Serang
Freie Universität Berlin and
Leibniz-Institute of Freshwater Ecology and Inland Fisheries (IGB)
orserang@uw.edu

December 4, 2021

Abstract

Max-convolution is an important problem closely resembling standard convolution; as such, max-convolution occurs frequently across many fields. Here we extend the method with fastest known worst-case runtime, which can be applied to nonnegative vectors by numerically approximating the Chebyshev norm $\|\cdot\|_\infty$, and derive a more accurate method. The absolute error of the proposed method is bounded and the runtime is demonstrated to be in $O(k \log_2(k) \log_2(\log_2(k)))$. The method is then used to approximate the Viterbi path in a hidden Markov with additive transitions; the runtime of approximating the Viterbi path is reduced from $O(nk^2)$ steps to $O(nk \log(k) \log(\log(k)))$ steps.

1 Introduction

Max-convolution occurs frequently in signal processing and Bayesian inference: it is used in image analysis[5], in network calculus[1], in economic equilibrium analysis[9], and in a probabilistic variant of combinatoric generating functions, wherein information on a sum of values into their most probable constituent parts (*e.g.* identifying proteins from mass spectrometry[6, 8]). Max-convolution operates on the semi-ring (\max, \times) , meaning that it behaves identically to a standard convolution, except it employs a max operation in lieu of the $+$ operation in standard convolution (max-convolution is also equivalent to min-convolution, also called infimal convolution, which operates on the tropical semi-ring $(\min, +)$). Due to the importance and ubiquity of max-convolution, sub-

stantial effort has been invested into highly optimized implementations (*e.g.*, implementations of the quadratic method on GPUs[10]).

Max-convolution can be defined using vectors (or discrete random variables, whose probability mass functions are analogous to nonnegative vectors) with the relationship $M = L + R$. Given the target sum $M = m$, the max convolution finds the values $L[\ell]$ and $R[r]$ for which $m = \ell + r$.

$$\begin{aligned} M[m] &= \max_{\ell, r: m=\ell+r} L[\ell]R[r] \\ &= \max_{\ell} L[\ell]R[m-\ell] \\ &= L *_{\max} R \end{aligned}$$

where $*_{\max}$ denotes the max-convolution operator. In probabilistic terms, this is equivalent to finding the highest probability of the joint events $\Pr(L = \ell, R = r)$ that would produce each possible value of the sum $M = L + R$ (note that in the probabilistic version, the vector M would subsequently need to be normalized so that its sum is 1).

Although applications of max-convolution are numerous, only a small number of methods exist for solving it[7]. These methods fall into two main categories, each with their own drawbacks: The first category consists of very accurate methods that have worst-case runtimes either quadratic[3] or slightly more efficient than quadratic in the worst-case[2]. Conversely, the second type of method computes a numerical approximation to the desired result, but in $O(k \log_2(k))$ steps; however, no bound for the numerical accuracy of this method has been derived[7].

While the two approaches from the first category of methods for solving max-convolution do so by either using complicated sorting routines or by creating a bijection to an optimization problem, the numerical approach solves max-convolution by showing an equivalence between $*_{\max}$ and the process of first generating a vector $u^{(m)}$ for each index m of the result (where $u^{(m)}[\ell] = L[\ell]R[m-\ell]$ for all in-bounds indices) and subsequently computing the maximum $M[m] = \max_{\ell} u^{(m)}[\ell]$. When L and R are nonnegative, the maximization over the vector $u^{(m)}$ can be computed exactly via the Chebyshev norm

$$\begin{aligned} M[m] &= \max_{\ell} u^{(m)}[\ell] \\ &= \lim_{p \rightarrow \infty} \|u^{(m)}\|_p \end{aligned}$$

but requires $O(k^2)$ steps (where k is the length of vectors L and R). However, once a fixed p^* -norm is chosen, then the approximation corresponding to that

p^* can be computed by expanding the p^* -norm to yield

$$\begin{aligned}
\lim_{p \rightarrow \infty} \|u^{(m)}\|_p &= \lim_{p \rightarrow \infty} \left(\sum_{\ell} \left(u^{(m)}[\ell] \right)^p \right)^{\frac{1}{p}} \\
&\approx \left(\sum_{\ell} \left(u^{(m)}[\ell] \right)^{p^*} \right)^{\frac{1}{p^*}} \\
&= \left(\sum_{\ell} L[\ell]^{p^*} R[r - \ell]^{p^*} \right)^{\frac{1}{p^*}} \\
&= \left(\sum_{\ell} \left(L^{p^*} \right)[\ell] \left(R^{p^*} \right)[r - \ell] \right)^{\frac{1}{p^*}} \\
&= \left(L^{p^*} * R^{p^*} \right)^{\frac{1}{p^*}}
\end{aligned}$$

where $L^{(p^*)} = \langle (L[0])^{p^*}, (L[1])^{p^*}, \dots, (L[k-1])^{p^*} \rangle$ and $*$ denotes standard convolution. The standard convolution can be done via fast Fourier transform (FFT) in $O(k \log_2(k))$ steps, which is substantially more efficient than the $O(k^2)$ required by the naive method (algorithm 1).

To date, the numerical method has currently demonstrated the best speed-accuracy trade-off on Bayesian inference tasks, and can be generalized to multiple dimensions (*i.e.*, tensors). In particular, they have been used with probabilistic convolution trees[6] to efficiently compute the most probable values of discrete random variables X_0, X_1, \dots, X_{n-1} for which the sum is known $X_0 + X_1 + \dots + X_{n-1} = y$ [6]. The one-dimensional variant of this problem (*i.e.*, where each X_i is a one-dimensional vector) solves the probabilistic generalization of the subset sum problem, while the two-dimensional variant (*i.e.*, where each X_i is a one-dimensional matrix) solves the generalization of the knapsack problem (note that these problems are not NP-hard in this specific case, because we assume an evenly-spaced discretization of the possible values of the random variables).

However, despite the practical performance that has been demonstrated by the numerical method, only cursory analysis has been performed to formalize the influence of the value of p^* on the accuracy of the result and to bound the error of the p^* -norm approximation. Optimizing the choice of p^* is non-trivial: Larger values of p^* more closely resemble a true maximization under the p^* -norm, but result in underflow (note that in **algorithm 1**, the maximum values of both L and R can be divided out and then multiplied back in after max-convolution so that overflow is not an issue). Conversely, smaller values of p^* suffer less underflow, but compute a norm with less resemblance to maximization. Here we perform an in-depth analysis of the influence of p^* on the accuracy of numerical max-convolution, and from that analysis we construct a modified piecewise algorithm, on which we demonstrate bounds on the worst-case absolute error. This modified algorithm, which runs in $O(k \log_2(k) \log_2(\log_2(k)))$

steps, is demonstrated using a hidden Markov model describing the relationship between U.S. unemployment and the S&P 500 stock index.

2 Methods

We begin by outlining and comparing three numerical methods for max-convolution. By analyzing the benefits and deficits of each of these methods, we create improved variants. All of these methods will make use of the basic numerical max-convolution idea summarized in the introduction, and as such we first declare a method for computing the numerical max-convolution estimate for a given p^* as `numericalMaxConvolveGivenPStar` (**algorithm 1**).

Algorithm 1 Numerical max-convolution given a fixed p^* , a numerical method to estimate the max-convolution of two PMFs or nonnegative vectors. The parameters are two nonnegative vectors L' and R' (both scaled so that they have maximal element 1) and the numerical value p^* used for computation. The return value is a numerical estimate of the max-convolution $L' *_{\max} R'$.

```

1: procedure NUMERICALMAXCONVOLVEGIVENPSTAR( $L', R', p^*$ )
2:    $\forall \ell, vL[\ell] \leftarrow L[\ell]^{p^*}$ 
3:    $\forall r, vR[r] \leftarrow R[r]^{p^*}$ 
4:    $vM \leftarrow vL * vR$  ▷ Standard FFT convolution is used here
5:    $\forall m, M'[m] \leftarrow vM[m]^{\frac{1}{p^*}}$ 
6:   return  $M'$ 
7: end procedure

```

Fixed low-value $p^* = 8$ method: The effects of underflow will be minimal (as it is not very far from standard FFT convolution, an operation with high numerical stability), but it can still be imprecise due to numerical “bleed-in” (*i.e.* error due to contributions from non-maximal terms for a given $u^{(m)}$ because the p^* -norm is not identical to the Chebyshev norm). Overall, this will perform well on indices where the exact value of the result is small, but perform poorly when the exact value of the result is large.

Fixed high-value $p^* = 64$ method: As noted above, will offer the converse pros and cons compared to using a low p^* : numerical artifacts due to bleed-in will be smaller (thus achieving greater performance on indices where the exact values of the result are larger), but underflow may be significant (and therefore, indices where the exact results of the max-convolution are small will be inaccurate).

Higher-order piecewise method: The higher-order piecewise method formalizes the empirical cutoff values found in Serang 2015; previously, numerical stability boundaries were found for each p^* by computing both the exact max-convolution (via the naive $O(k^2)$ method) and via the numerical method using

the ascribed value of p^* , and finding the value below which the numerical values experienced a high increase in relative absolute error.

Those previously observed empirical numerical stability boundaries can be formalized by using the fact that the employed `numpy` implementation of FFT convolution has high accuracy on indices where the result has a value $\geq \tau$ relative to the maximum value; therefore, if the arguments L and R are both normalized so that each has a maximum value of 1, the fast max-convolution approximation is numerically stable for any index m where the result of the FFT convolution, *i.e.* $vM[m]$, is $\geq \tau$. The `numpy` documentation defines the machine precision $\tau = 10^{-14}$, which corresponds well with the boundary points demonstrated in **figure 1**.

Because Cooley-Tukey implementations of FFT-based convolution (*e.g.*, the `numpy` implementation) are widely applied to large problems with extremely small error, we will make a simplification and assume that the FFT has perfect accuracy on indices where the result of the convolution is $\geq p^*$, even though it is also a numerical method and is subject to small inaccuracies. Therefore, from this point forward, we use a slightly more conservative $\tau = 10^{-13}$ and consider that the dominant cause of error to come from the max-convolution approximation (*i.e.*, employing $\|u^{(m)}\|_{p^*}$ instead of $\|u^{(m)}\|_\infty$). Using larger p^* values will provide a closer approximation; however, using a larger value of p^* may also drive values to zero (because the inputs L and R will be normalized within **algorithm 1** so that the maximum of each is 1 when convolved via FFT), limiting the indices to those m for which $vM[m] \geq \tau$.

The choice of p^* can be characterized by two opposing sources of error: higher p^* values better approximate $\|u^{(m)}\|_{p^*}$ but will be numerically unstable for many indices; lower p^* values provide worse approximations of $\|u^{(m)}\|_{p^*}$ but will be numerically unstable for only few indices. These opposing sources of error pose a natural method for improving the accuracy of this max-convolution approximation. By considering a small collection of p^* values, we can compute the full numerical estimate (at all indices) with each p^* using **algorithm 1**; computing the full result at a given p^* is $\in O(k \log_2(k))$, so doing so on some small number c of p^* values considered, then the overall runtime will be $\in O(ck \log_2(k))$. Then, a final estimate is computed at each index by using the largest p^* that is stable (with respect to underflow) at that index. Choosing the largest p^* (of those that are stable with respect to underflow) corresponds to minimizing the bleed-in error, because the larger p^* becomes, the more muted the non-maximal terms in the norm become (and thus the closer the p^* -norm becomes to the true maximum).

Here we introduce this piecewise method and compare it to the simpler low-value $p^* = 8$ and high-value $p^* = 64$ methods and analyze the worst-case error of the piecewise method.

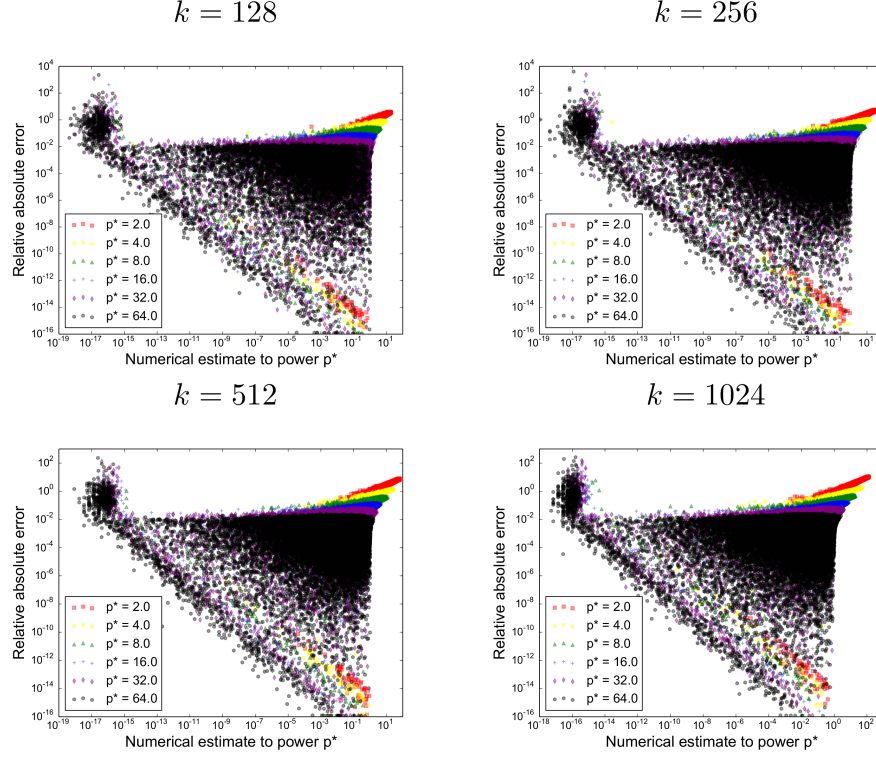


Figure 1: **Empirical estimate of τ to construct a piecewise method.** For each $k \in \{128, 256, 512, 1024\}$, 32 replicate max-convolutions (on vectors filled with uniform values) are performed. Error from two sources can be seen: error due to underflow is depicted in the sharp left mode, whereas error due to imperfect approximation, where $\|\cdot\|_{p^*} > \|\cdot\|_\infty$ can be seen in the gradual mode on the right. Error due to p^* -norm approximation is significantly smaller when p^* is larger (thereby flattening the right mode), but larger p^* values are more susceptible to underflow, pushing more indices into the left mode. Regardless of the value of k , error due to underflow occurs when $(\|\cdot\|_{p^*})^{p^*}$ goes below $\approx 10^{-14}$; this matches the numerical tolerance for τ described by the `numpy` documentation. Therefore, at each index m we can construct a piecewise method that uses the largest value of p^* for which $\|u^{(m)}\|_{p^*}^{p^*} \geq \tau$.

Algorithm 2 Piecewise numerical max-convolution , a numerical method to estimate the max-convolution nonnegative vectors (revised to reduce bleed-in error). This procedure uses a p^* close to the largest possible stable value at each result index. The return value is a numerical estimate of the max-convolution $L *_{\max} R$. The runtime is in $O(k \log_2(k) \log_2(p_{\max}^*))$.

```

1: procedure NUMERICALMAXCONVOLVEPIECEWISE( $L, R, p_{\max}^*$ )
2:    $\ell_{\max} \leftarrow \operatorname{argmax}_{\ell} L[\ell]$ 
3:    $r_{\max} \leftarrow \operatorname{argmax}_r R[r]$ 
4:    $L' \leftarrow \frac{L}{L[\ell_{\max}]}$ 
5:    $R' \leftarrow \frac{R}{R[r_{\max}]}$  ▷ Scale to a proportional problem on  $L', R'$ 
6:    $allPStar \leftarrow [2^0, 2^1, \dots, 2^{\lceil \log_2(p_{\max}^*) \rceil}]$ 
7:   for  $i \in \{0, 1, \dots, \operatorname{len}(allPStar) - 1\}$  do
8:      $resForAllPStar[i] \leftarrow \operatorname{fftNonnegMaxConvolveGivenPStar}(L', R',$ 
        $allPStar[i])$ 
9:   end for
10:  for  $m \in \{0, 1, \dots, \operatorname{len}(L) + \operatorname{len}(R) - 1\}$  do
11:     $maxStablePStar[m] \leftarrow \max\{i : (\operatorname{resForAllPStar}[i][m])^{allPStar[i]} \geq \tau\}$ 
12:  end for
13:  for  $m \in \{0, 1, \dots, \operatorname{len}(L) + \operatorname{len}(R) - 1\}$  do
14:     $i \leftarrow maxStablePStar[m]$ 
15:     $result[m] \leftarrow resForAllPStar[i][m]$ 
16:  end for
17:  return  $L[\ell_{\max}] \times R[r_{\max}] \times result$  ▷ Undo previous scaling
18: end procedure

```

3 Results

3.1 Error and runtime analysis of the piecewise method

Error analysis for a fixed underflow-stable p^* : We first scale L and R into L' and R' respectively, where the maximum elements of both L' and R' are 1; the absolute error can be found by unscaling the absolute error of the scaled problem:

$$\begin{aligned} & |exact(L, R)[m] - numeric(L', R')[m]| \\ &= \max_{\ell} L[\ell] \max_r R[r] |exact(L', R')[m] - numeric(L', R')[m]|. \end{aligned}$$

We first derive an error bound for the scaled problem on L', R' (any mention of a vector $u^{(m)}$ refers to the scaled problem), and then reverse the scaling to demonstrate the error bound on the original problem on L, R .

For any particular “underflow-stable” p^* (*i.e.*, any value of p^* for which $(\|u^{(m)}\|_{p^*})^{p^*} \geq \tau$), the absolute error for the numerical method for fast max-convolution can be bound fairly easily by factoring out the maximum element of $u^{(m)}$ (this maximum element is equivalent to the Chebyshev norm) from the p^* -norm:

$$\begin{aligned} & |exact(L', R')[m] - numeric(L', R')[m]| \\ &= |||u^{(m)}\|_{p^*} - \|u^{(m)}\|_{\infty}| \\ &= \|u^{(m)}\|_{p^*} - \|u^{(m)}\|_{\infty} \\ &= \|u^{(m)}\|_{\infty} \left(\frac{\|u^{(m)}\|_{p^*}}{\|u^{(m)}\|_{\infty}} - 1 \right) \\ &= \|u^{(m)}\|_{\infty} \left(\left\| \frac{u^{(m)}}{\|u^{(m)}\|_{\infty}} \right\|_{p^*} - 1 \right) \\ &= \|u^{(m)}\|_{\infty} \left(\|v^{(m)}\|_{p^*} - 1 \right) \end{aligned}$$

where $v^{(m)}$ is a nonnegative vector of the same length as $u^{(m)}$ (this length is denoted k_m) where $v^{(m)}$ contains one element equal to 1 (because the maximum element of $u^{(m)}$ must, by definition, be contained within $u^{(m)}$) and where no element of $v^{(m)}$ is greater than 1 (also provided by the definition of the maximum).

$$\begin{aligned} \|v^{(m)}\|_{p^*} &\leq \| \langle 1, 1, \dots, 1 \rangle \|_{p^*} \\ &= \left(\sum_i^{k_m} 1^{p^*} \right)^{\frac{1}{p^*}} \\ &= k_m^{\frac{1}{p^*}} \end{aligned}$$

Thus the error is bound:

$$\begin{aligned}
& |exact(L', R')[m] - numeric(L', R')[m]| \\
&= \|u^{(m)}\|_\infty \left(v^{(m)}\|_{p^*} - 1 \right) \\
&\leq \|v^{(m)}\|_{p^*} - 1 \\
&\leq k_m^{\frac{1}{p^*}} - 1,
\end{aligned}$$

because $\forall m, \|u^{(m)}\|_\infty \leq 1$ for a scaled problem on L', R' .

Error analysis of piecewise method: However, the bounds derived above are only applicable for p^* where $(\|u^{(m)}\|_{p^*})^{p^*} \geq \tau$. The piecewise method is slightly more complicated, and can be partitioned into two cases: In the first case, the top contour is used (*i.e.*, when p_{\max}^* is underflow-stable). Conversely, in the second case, a middle contour is used (*i.e.*, when p_{\max}^* is not underflow-stable).

In the first case, when we use the top contour $p^* = p_{\max}^*$, we know that p_{\max}^* must be underflow-stable, and thus we can reuse the bound given an underflow-stable p^* .

In the second case, because the p^* used is $< p_{\max}^*$, it follows that the next higher contour (using $2p^*$) must not be underflow-stable (because the highest underflow-stable p^* is used and because the p^* are searched in log-space). The bound derived above that demonstrated

$$\|u^{(m)}\|_{p^*} \leq \|u^{(m)}\|_\infty k_m^{\frac{1}{p^*}}$$

can be combined with the property that $\|\cdot\|_{p^*} > \|\cdot\|_\infty$ for any $p^* \geq 1$ to show that

$$\|u^{(m)}\|_\infty \in \left[\frac{\|u^{(m)}\|_{p^*}}{k_m^{\frac{1}{p^*}}}, \|u^{(m)}\|_{p^*} \right].$$

Thus the absolute error can be bound again using the fact that we are in a middle contour:

$$\begin{aligned}
&= \|u^{(m)}\|_{p^*} - \|u^{(m)}\|_\infty \\
&= \|u^{(m)}\|_{p^*} \left(1 - \frac{\|u^{(m)}\|_\infty}{\|u^{(m)}\|_{p^*}} \right) \\
&\leq \|u^{(m)}\|_{p^*} \left(1 - k_m^{\frac{-1}{p^*}} \right) \\
&< \tau^{\frac{1}{2p^*}} \left(1 - k_m^{\frac{-1}{p^*}} \right).
\end{aligned}$$

The absolute error from middle contours will be quite small when $p^* = 1$ is the maximum underflow-stable value of p^* at index m , because $\tau^{\frac{1}{2p^*}}$, the

first factor in the error bound, will become $\sqrt{\tau} \approx 10^{-6}$, and $1 - k_m^{\frac{-1}{p^*}} < 1$ (qualitatively, this indicates that a small p^* is only used when the result is very close to zero, leaving little room for absolute error). Likewise, when a very large p^* is used, then $1 - k_m^{\frac{-1}{p^*}}$ becomes very small, while $\tau^{\frac{1}{2p^*}} < 1$ (qualitatively, this indicates that when a large p^* is used, the $\|\cdot\|_{p^*} \approx \|\cdot\|_\infty$, and thus there is little absolute error). Thus for the extreme values of p^* , middle contours will produce fairly small absolute errors. The unique mode p_{mode}^* can be found by finding the value that solves

$$\frac{\partial}{\partial p_{mode}^*} \left(\tau^{\frac{1}{2p_{mode}^*}} \left(1 - k_m^{\frac{-1}{p_{mode}^*}} \right) \right) = 0,$$

which yields

$$p_{mode}^* = \frac{\log_2(k_m)}{\log_2\left(-\frac{2\log_2(k)-\log_2(\tau)}{\log_2(\tau)}\right)}.$$

An appropriate choice of p_{\max}^* should be $> p_{mode}^*$ so that the error for any contour (both middle contours and the top contour) are smaller than the error achieved at p_{mode}^* , allowing us to use a single bound for both. Choosing $p_{\max}^* = p_{mode}^*$ would guarantee that all contours are no worse than the middle-contour error at p_{mode}^* ; however, using $p_{\max}^* = p_{mode}^*$ is still quite liberal, because it would mean that for indices in the highest contour (there must be a nonempty set of such indices, because the scaling on L' and R' guarantees that the maximum index will have an exact value of 1, meaning that the approximation endures no underflow and is underflow-stable for every p^*), a better error *could* be achieved by increasing p_{\max}^* . For this reason, we choose p_{\max}^* so that the top-contour error produced at p_{\max}^* is not substantially larger than all errors produced for p^* before the mode (*i.e.*, for $p^* < p_{mode}^*$).

For this reason, we choose that the top-contour error at p_{\max}^* should not be much larger than the minimum error for any $p^* < p_{mode}^*$. The minimum worst-case middle-contour error will occur at $p^* = 1$, because the function is unimodal and increasing in the range $[1, p_{mode}^*)$. Therefore, we specify that the top-contour error at p_{\max}^* should be no more than the square-root of the middle-contour error at $p^* = 1$ and using the worst-case the length of $u^{(m)}$ is the full length of the L and R (*i.e.*, $k_m = k$). Solving

$$\sqrt{\tau} \left(1 - \frac{1}{k} \right) = k^{\frac{1}{p_{\max}^*}} - 1$$

yields

$$\begin{aligned} p_{mode}^* &= \frac{\log_2(k)}{\log_2(1 + \sqrt{\sqrt{\tau} \left(1 - \frac{1}{k} \right)})} \\ &\approx \frac{\log_2(k)}{\log_2(1 + \sqrt{\sqrt{\tau}})} \end{aligned}$$

for any non-trivial problem (*i.e.*, when $k \gg 1$), and thus

$$p_{\max}^* \approx \log_{1+\tau^{\frac{1}{4}}}(k),$$

indicating that the absolute error at the top contour will be roughly equal to the fourth root of τ .

Worst-case absolute error: By setting p_{\max}^* in this manner, we guarantee that the absolute error at any index of any unscaled problem on L, R is less than

$$\max_{\ell} L[\ell] \max_r R[r] \tau^{\frac{1}{2p_{\max}^*}} \left(1 - k_m^{\frac{-1}{p_{\max}^*}}\right)$$

where p_{\max}^* is defined above. The full formula for the middle-contour error at this value of p_{\max}^* does not simplify and is therefore quite large; for this reason, it is not reported here, but this gives a numeric bound of the worst case middle-contour error that is bound in terms of the variable k (and with no other variables free).

Runtime analysis: The piecewise method clearly performs $\log_2(p_{\max}^*)$ FFTs (each requiring $O(k \log_2(k))$ steps); therefore, since p_{\max}^* is chosen to be $\log_{1+\tau^{\frac{1}{4}}}(k)$ (to achieve the desired error bound), the total runtime is thus

$$O(k \log_2(k) \log_2(\log_{1+\tau^{\frac{1}{4}}}(k))).$$

For any practically sized problem, the $\log_2(\log_{1+\tau^{\frac{1}{4}}}(k))$ factor is essentially a constant; even when k is chosen to be the number of particles in the observable universe ($\approx 2^{270}$ [4]), the $\log_2(\log_{1+\tau^{\frac{1}{4}}}(k))$ is ≈ 18 , meaning that for any problem of practical size, the full piecewise method is no more expensive than computing 18 FFTs.

3.2 Comparison of low-value $p^* = 8$, high-value $p^* = 64$, and piecewise method

3.3 Improved affine piecewise method

Figure 2b depicts a scatter plot of the exact result vs. the piecewise approximation at every index (using the same problem from **figure 2a**) depicts a clear banding pattern: the exact and approximate results are clearly correlated, but each contour (*i.e.*, each collection of indices that use a specific p^*) has a different average slope between the exact and approximate values, with higher p^* contours showing a generally larger slope and smaller p^* contours showing greater spread and lower slopes; this intuitively makes sense, because the bounds on $\|u^{(m)}\|_{\infty} \in [\|u^{(m)}\|_{p^*} k_m^{\frac{-1}{p^*}}, \|u^{(m)}\|_{p^*}]$ derived above constrain the scatter plot points inside a quadrilateral envelope (**figure 3**).

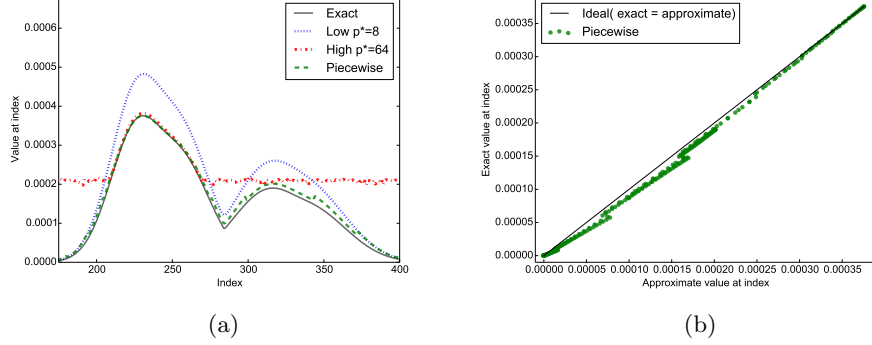


Figure 2: **The accuracy of numerical fast max-convolution methods.** **(a)** Different approximations for a sample max-convolution problem. The low- p^* method is underflow-stable, but overestimates the result. The high- p^* method is accurate when underflow-stable, but experiences underflow at many indices. The piecewise method stitches together approximations from different p^* to maintain underflow-stability. **(b)** Exact vs. piecewise approximation at various indices of the same problem. A clear banding pattern is observed with one tight, elliptical cluster for each contour. The slope of the clusters deviates more for the contours using lower p^* values.

The correlations within each contour can be exploited to correct biases that emerge for smaller p^* values. In order to do this, $\|u^{(m)}\|_\infty$ must be computed for at least two points m_1 and m_2 within the contour, so that a mapping $\|u^{(m)}\|_{p^*} \approx f(\|u^{(m)}\|_\infty) = a\|u^{(m)}\|_{p^*} + b$ can be constructed. Fortunately, a single $\|u^{(m)}\|_\infty$ can be computed exactly in $O(k)$ (by actually computing a single $u^{(m)}$ and computing its max, which is equivalent to computing a single index result via the naive quadratic method). As long as the exact value $\|u^{(m)}\|_\infty$ is computed for only a small number of indices, then the order of the runtime will not change (each contour already costs $O(k \log_2(k))$, so adding a small number of $O(k)$ steps for each contour will not change the runtime).

If the two indices chosen are

$$m_{\min} = \operatorname{argmin}_{m \in \text{contour}(p^*)} \|u^{(m)}\|_{p^*}$$

$$m_{\max} = \operatorname{argmax}_{m \in \text{contour}(p^*)} \|u^{(m)}\|_{p^*},$$

then we are guaranteed that the affine function f can be written as a convex combination of the exact values at those extreme points (using barycentric coordinates):

$$f(\|u^{(m)}\|_{p^*}) = \lambda_m \|u^{(m_{\max})}\|_\infty + (1 - \lambda_m) \|u^{(m_{\min})}\|_\infty$$

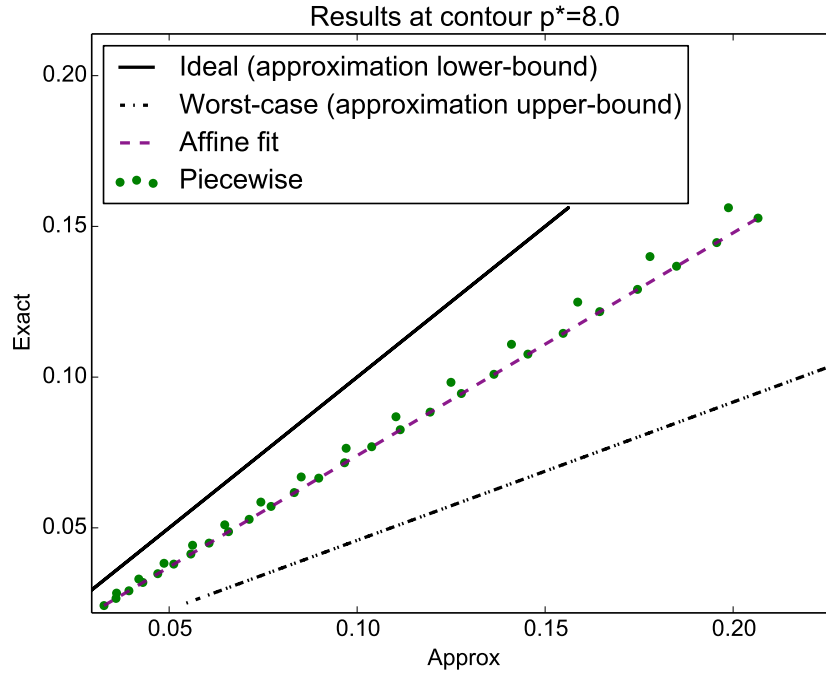


Figure 3: **A single contour from the piecewise approximation.** The cluster of points (one point for each index in the previous figure) is bound by the exact value (ideal approximation) and the approximation upper-bound for $p^* = 8$ (worst-case approximation). The points are well described by an affine function fit using the left-most and right-most points.

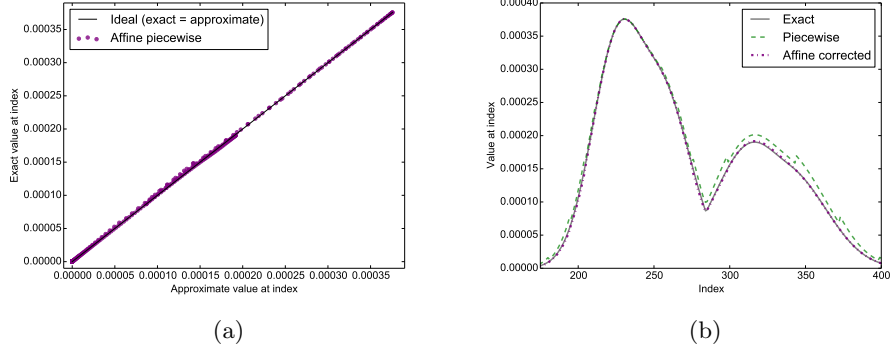


Figure 4: **Piecewise method with affine contour fitting.** The approximate values at each index of the max-convolution problem are almost identical to the exact result at the same index.

$$\lambda_m = \frac{\|u^{(m)}\|_{p^*} - \|u^{(m_{\min})}\|_{p^*}}{\|u^{(m_{\max})}\|_{p^*} - \|u^{(m_{\min})}\|_{p^*}} \in [0, 1]$$

Thus, by computing $\|u^{(m_{\min})}\|_{\infty}$ and $\|u^{(m_{\max})}\|_{\infty}$ (each in $O(k)$ steps), we can compute an affine function f to correct contour-specific trends (**algorithm 3**).

Error analysis of the improved affine piecewise method By exploiting the convex combination used to define f , the absolute error of the affine piecewise method can also be bound. Qualitatively, this is because, by fitting on the extrema in the contour, we are now interpolating. If the two points used to determine the parameters of the affine function were not chosen in this manner to fit the affine function, then it would be possible to choose two points with very close x-values (*i.e.*, similar approximate values) and disparate y-values (*i.e.*, different y-values), and extrapolating to other points could propagate a large slope over a large distance; using the extreme points forces the affine function to be a convex combination of the extrema, thereby avoiding this problem.

Algorithm 3 Improved affine piecewise numerical max-convolution, a numerical method to estimate the max-convolution nonnegative vectors (further revised to reduce numerical error). This procedure uses a p^* close to the largest possible stable value at each result index. The return value is a numerical estimate of the max-convolution $L *_{\max} R$. The runtime is in $O(k \log_2(k) \log_2(p_{\max}^*))$.

```

1: procedure NUMERICALMAXCONVOLVEPIECEWISEAFFINE( $L, R, p_{\max}^*$ )
2:    $\ell_{\max} \leftarrow \operatorname{argmax}_{\ell} L[\ell]$ 
3:    $r_{\max} \leftarrow \operatorname{argmax}_r R[r]$ 
4:    $L' \leftarrow \frac{L}{L[\ell_{\max}]}$ 
5:    $R' \leftarrow \frac{R}{R[r_{\max}]}$  ▷ Scale to a proportional problem on  $L', R'$ 
6:    $\text{allPStar} \leftarrow [2^0, 2^1, \dots, 2^{\lceil \log_2(p_{\max}^*) \rceil}]$ 
7:   for  $i \in \{0, 1, \dots, \text{len}(\text{allPStar})\}$  do
8:      $\text{resForAllPStar}[i] \leftarrow \text{fftNonnegMaxConvolveGivenPStar}(L', R',$ 
        $\text{allPStar}[i])$ 
9:   end for
10:  for  $m \in \{0, 1, \dots, \text{len}(L) + \text{len}(R) - 1\}$  do
11:     $\text{maxStablePStar}[m] \leftarrow \max\{i : (\text{resForAllPStar}[i][m])^{\text{allPStar}[i]} \geq \tau\}$ 
12:  end for
13:   $\forall i, \text{slope}[i] \leftarrow 1$ 
14:   $\forall i, \text{bias}[i] \leftarrow 0$ 
15:   $\text{usedPStar} \leftarrow \text{set}(\text{maxStablePStar})$ 
16:  for  $i \in \text{usedPStar}$  do
17:     $\text{contour} \leftarrow \{m : \text{maxStablePStar}[m] = i\}$ 
18:     $mMin \leftarrow \operatorname{argmin}_{m \in \text{contour}} \text{resForAllPStar}[i][m]$ 
19:     $mMax \leftarrow \operatorname{argmax}_{m \in \text{contour}} \text{resForAllPStar}[i][m]$ 
20:     $xMin \leftarrow \text{resForAllPStar}[i][mMin]$ 
21:     $xMax \leftarrow \text{resForAllPStar}[i][mMax]$ 
22:     $yMin \leftarrow \text{maxConvolutionAtIndex}(mMin)$ 
23:     $yMax \leftarrow \text{maxConvolutionAtIndex}(mMax)$ 
24:    if  $xMax > xMin$  then
25:       $\text{slope}[i] \leftarrow \frac{yMax - yMin}{xMax - xMin}$ 
26:       $\text{bias}[i] \leftarrow yMin - \text{slope}[i] \times xMin$ 
27:    else
28:       $\text{slope}[i] \leftarrow \frac{yMax}{xMax}$ 
29:    end if
30:  end for
31:  for  $m \in \{0, 1, \dots, \text{len}(L) + \text{len}(R) - 1\}$  do
32:     $i \leftarrow \text{maxStablePStar}[m]$ 
33:     $\text{result}[m] \leftarrow \text{resForAllPStar}[i][m] \times \text{slope}[i] + \text{bias}[i]$ 
34:  end for
35:  return  $L[\ell_{\max}] \times R[r_{\max}] \times \text{result}$  ▷ Undo previous scaling
36: end procedure

```

$$\begin{aligned}
f(\|u^{(m)}\|_{p^*}) &= \lambda_m \|u^{(m_{\max})}\|_{\infty} + (1 - \lambda_m) \|u^{(m_{\min})}\|_{\infty} \\
&\in \left[\lambda_m \frac{\|u^{(m_{\max})}\|_{p^*}}{k^{\frac{1}{p^*}} m_{\max}^{\frac{1}{p^*}}} + (1 - \lambda_m) \frac{\|u^{(m_{\min})}\|_{p^*}}{k^{\frac{1}{p^*}} m_{\min}^{\frac{1}{p^*}}}, \right. \\
&\quad \left. \lambda_m \|u^{(m_{\max})}\|_{p^*} + (1 - \lambda_m) \|u^{(m_{\min})}\|_{p^*} \right] \\
&\subseteq \left[\lambda_m \frac{\|u^{(m_{\max})}\|_{p^*}}{k^{\frac{1}{p^*}}} + (1 - \lambda_m) \frac{\|u^{(m_{\min})}\|_{p^*}}{k^{\frac{1}{p^*}}}, \right. \\
&\quad \left. \lambda_m \|u^{(m_{\max})}\|_{p^*} + (1 - \lambda_m) \|u^{(m_{\min})}\|_{p^*} \right] \\
&= \left[k^{\frac{-1}{p^*}} \left(\lambda_m \|u^{(m_{\max})}\|_{p^*} + (1 - \lambda_m) \|u^{(m_{\min})}\|_{p^*} \right), \right. \\
&\quad \left. \lambda_m \|u^{(m_{\max})}\|_{p^*} + (1 - \lambda_m) \|u^{(m_{\min})}\|_{p^*} \right] \\
&= \left[k^{\frac{-1}{p^*}} \|u^{(m)}\|_{p^*}, \|u^{(m)}\|_{p^*} \right]
\end{aligned}$$

The worst-case absolute error of the scaled problem on L', R' can be defined

$$\max_m |f(\|u^{(m)}\|_{p^*}) - \|u^{(m)}\|_{\infty}|.$$

Because the function $f(\|u^{(m)}\|_{p^*}) - \|u^{(m)}\|_{\infty}$ is affine, its derivative can never be zero, and thus Lagrangian theory states that the maximum must occur at a boundary point. Therefore, the worst-case absolute error is

$$\begin{aligned}
&\leq \max\{\|u^{(m)}\|_{p^*} - \|u^{(m)}\|_{\infty}, \|u^{(m)}\|_{\infty} - \|u^{(m)}\|_{p^*} k^{\frac{-1}{p^*}}\} \\
&= \|u^{(m)}\|_{p^*} - \|u^{(m)}\|_{\infty},
\end{aligned}$$

which is identical to the worst-case error bound before applying the affine transformation f . Thus applying the affine transformation can dramatically improve error, but will not make it worse than the original worst-case.

3.4 Demonstration on hidden Markov model with additive transitions

One example that profits from fast max-convolution of non-negative vectors is computing the Viterbi path using a hidden Markov model (HMM) (*i.e.*, the *maximum a posteriori* states) with an additive transition function satisfying $\Pr(X_{i+1} = a | X_i = b) \propto \delta(a - b)$ for some arbitrary function δ (δ can be represented as a table, because we are considering all possible discrete functions). Because of the Markov property of the chain, we only need to max-marginalize out the latent variable at time i to compute the distribution for the next latent variable X_{i+1} and all observed values of the data variables $D_0 \dots D_{i+1}$. This procedure, called the Viterbi algorithm, is continued inductively:

$$\begin{aligned}
& \max_{x_0, x_1, \dots, x_{i-1}} \Pr(D_0, D_1, \dots, D_{i-1}, X_0 = x_0, X_1 = x_1, \dots, X_i = x_i) = \\
& \max_{x_{i-1}} \max_{x_0, x_1, \dots, x_{i-2}} \Pr(D_0, D_1, \dots, D_{i-2}, X_0 = x_0, X_1 = x_1, \dots, X_{i-1} = x_{i-1}) \\
& \Pr(D_{i-1} | X_{i-1} = x_{i-1}) \Pr(X_i = x_i | X_{i-1} = x_{i-1})
\end{aligned}$$

and continuing by exploiting the self-similarity on a smaller problem to proceed inductively, revealing a max-convolution (for this specialized HMM with additive transitions):

$$\begin{aligned}
& = \max_{x_{i-1}} \text{fromLeft}[i - 1] \Pr(D_{i-1} | X_{i-1} = x_{i-1}) \delta[x_i - x_{i-1}] = \\
& (\text{fromLeft}[i - 1] \text{likelihood}[D_{i-1}]) *_{\max} \delta[x_i - x_{i-1}].
\end{aligned}$$

After computing this left-to-right pass (which consisted of $n - 1$ max-convolutions and vector multiplications), we can find the *maximum a posteriori* configuration of the latent variables $X_0, \dots, X_{n-1} = x_0^*, \dots, x_{n-1}^*$ backtracking right-to-left, which can be done by finding the variable value x_i that maximizes $\text{fromLeft}[i][x_i] \times \delta[x_{i+1}^* - x_i]$ (thus defining x_i^* and enabling induction on the right-to-left pass). The right-to-left pass thus requires $O(nk)$ steps (**algorithm 4**). Note that the full max-marginal distributions on each latent variable X_i can be computed via a small modification, which would perform a more complex right-to-left pass that is nearly identical to the left-to-right pass, but which performs subtraction instead of addition (*i.e.*, by reversing the vector representation of the PMF of the subtracted argument before it is max-convolved)[6].

We apply this HMM with additive transition probabilities to a data analysis problem from economics. It is known for example, that the current figures of unemployment in a country have (among others) impact on prices of commodities like oil. If one could predict unemployment figures before the usual weekly or monthly release by the responsible government bureaus, this would lead to an information advantage and an opportunity for short-term arbitrage. Economic indicators like market prices and stock market indices (especially of indices combining several stocks of different industries) are closely related with unemployment statistics.

In the following demonstration of our method, we create a simple HMM with additive transitions and use it to infer the *maximum a posteriori* unemployment statistics given past history (*i.e.* how often unemployment is low and high, as well as how often unemployment goes down or up in a short amount of time) and current stock market prices (the observed data). We discretized random variables for the observed data (S&P 500, adjusted closing prices (retrieved from YAHOO! historical stock prices: <http://data.bls.gov/cgi-bin/>

Algorithm 4 ViterbiForModelWithAdditiveTransitions, which accepts the k -length vector $prior$, a list of n binned observations $data$, a $c \times k$ matrix of likelihoods (where c is the number of bins used to discretize the data) $likelihoods$, and a $2k$ -length vector δ that describes the transition probabilities. The algorithm returns a Viterbi path of length n , where each element in the path is a valid state $\in \{0, 1, \dots, k-1\}$.

```

1: procedure VITERBIFORADDITIVETRANSITIONS( $prior, data, likelihood, \delta$ )
2:    $fromLeft[0] \leftarrow prior$ 
3:   for  $i = 0$  to  $n - 2$  do
4:      $fromLeft[i] \leftarrow fromLeft[i] \times likelihood[data[i]]$ 
5:      $fromLeft[i + 1] \leftarrow fromLeft[i] *_{\max} \delta$ 
6:   end for
7:    $fromLeft[n] \leftarrow fromLeft[n] \times likelihood[data[n]]$ 
8:
9:    $path[n] \leftarrow \operatorname{argmax}_j fromLeft[n][j]$ 
10:  for  $i = n - 1$  to  $0$  do
11:     $maxProdPosterior \leftarrow -1$ 
12:     $argmaxProdPosterior \leftarrow -1$ 
13:    for  $l = k$  to  $1$  do
14:       $currProdPosterior \leftarrow fromLeft[i] \times \delta[l - path[i + 1]]$ 
15:      if  $currProdPosterior > maxProdPosterior$  then
16:         $maxProdPosterior \leftarrow currProdPosterior$ 
17:         $argmaxProdPosterior \leftarrow l$ 
18:      end if
19:    end for
20:     $path[i] \leftarrow argmaxProdPosterior$ 
21:  end for
22:  return  $path$ 
23: end procedure

```

survey`most?blsseriesCUUR0000SA0`), inflation adjusted by (*i.e.* divided by) consumer price index (CPI) (retrieved from the U.S. Bureau of Labor Statistics: <https://finance.yahoo.com/q?s=GSPC>) and "latent" variables (unemployment insurance claims, seasonally adjusted, were retrieved from the U.S. Department of Labor: <https://www.oui.doleta.gov/unemploy/claims.asp>). Data was available weekly from week 4 in 1967 to week 52 in 2014, resulting in 2500 data points for each type of variable.

To investigate the influence of overfitting, we partition the data in two parts, before June 2005 and after June 2005, so that we are effectively training on $2000 * 100 / 2500 = 80\%$ of the data points, and then demonstrate the Viterbi path on the entirety of the data (both the 80% training data and the 20% of the data withheld from empirical parameter estimation). Unemployment insurance claims were discretized into 512 and stock prices were discretized into 128 bins. A simple empirical model of the prior distribution for unemployment, the likelihood of unemployment given stock prices, and the transition probability of unemployment were built as follows: The initial or prior distribution for unemployment claims at $i = 0$ was calculated by marginalizing the time series of training data for the claims (*i.e.* counting the number of times any particular unemployment value was reached over all possible bins). Our transition function (the conditional probability $\Pr(X_{i+1}|X_i)$) similarly counts the number of times each possible change $X_{i+1} - X_i \in \{510, 509, \dots, 511\}$ occurred over all available time points. Interestingly, the resulting transition distribution roughly resembles a Gaussian (but is not an exact Gaussian). This underscores a great quality of working with discrete distributions: while continuous distributions may have closed forms for max-convolution (which can be computed quickly), discrete distributions have the distinct advantage that they can accurately approximate any smooth distribution. Lastly, the likelihoods of observing a stock price given the unemployment at the same time were trained using an empirical joint distribution (essentially a heatmap), which is displayed in **figure 5**.

We compute the Viterbi path two times: First we use naive, exact max-convolution, which requires a total of $O(nk^2)$ steps. Second, we use fast numerical max-convolution, which requires $O(n k \log(k) \log(\log(k)))$ steps. Despite the simplicity of the model, the exact Viterbi path (computed via exact max-convolution) is highly informative for predicting the value of unemployment, even for the 20% of the data that were not used to estimate the empirical prior, likelihood, and transition distributions. Also, the numerical max-convolution method is nearly identical to the exact max-convolution method at every index (**figure 6**). Even with a fairly rough discretization (*i.e.*, $k = 512$), the fast numerical method used 84.11 seconds compared to the 221.84 seconds required by the naive approach. This speedup will increase dramatically as k is increased, because the $\log(\log(k))$ term in the runtime of the numerical max-convolution method is essentially bounded above $\log(\log(k)) \leq 18$.

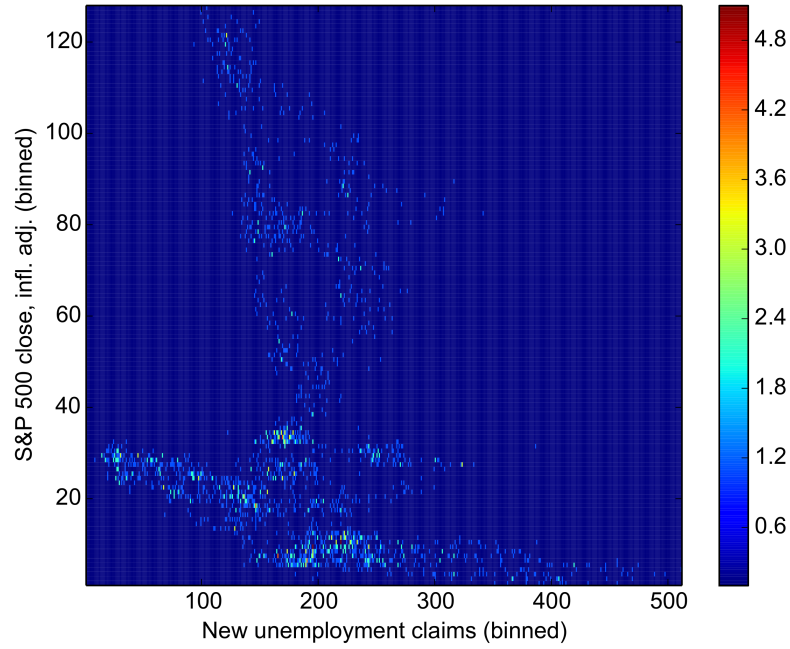


Figure 5: **Heatmap for trained likelihood matrix.** This heatmap depicts a joint empirical distribution between the S& P 500 index and new unemployment claims, which share a tenuous inverse relationship. Given D_i , the discretized stock index value at time i , row D_i contains the likelihood table $\Pr(D_i|X_i)$, which is denoted `likelihood[data[i]]` in the code.

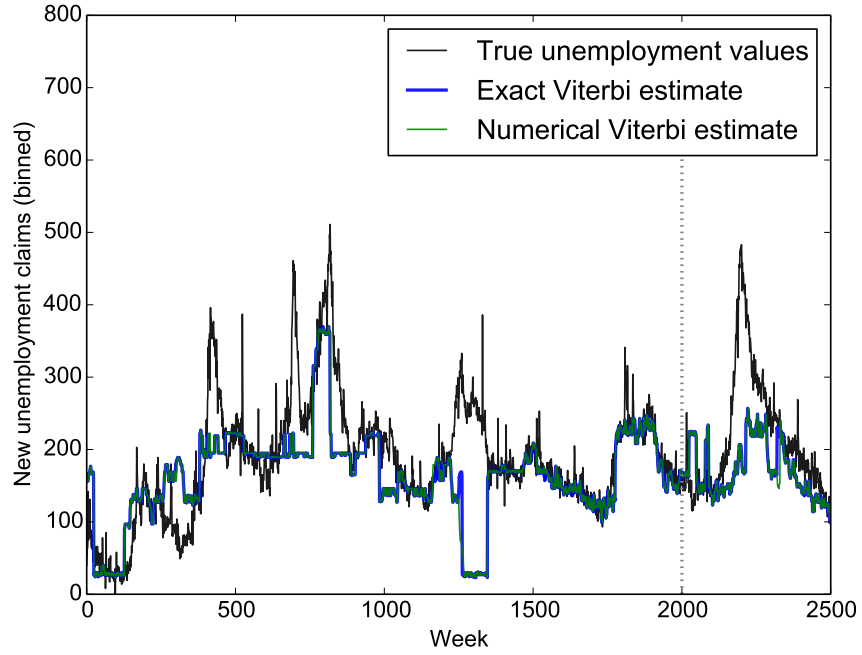


Figure 6: **Viterbi analysis of employment given stock index values.** The Viterbi path corresponding to the *maximum a posteriori* prediction of the number of new unemployment insurance claims is produced for a model where the state transition probabilities are additive. The exact Viterbi estimate tracks well with the true unemployment values. Training parameters were taken from only the true unemployment data to the left of the vertical dotted line; however, the Viterbi paths to the right of the dotted line (where unemployment data were withheld from the likelihood, prior, and transition parameters) also track well with the true unemployment statistics. The Viterbi path computed with fast numerical max-convolution (via the affine piecewise approach) is nearly identical to the result computed with the slower exact approach.

4 Discussion

The proposed numerical method is highly accurate in practice and achieves a substantial speedup over the naive approach. This is particularly true for large problems, because although the $\log_2(\log_{1+\tau^{\frac{1}{4}}}(k))$ multiplier may never be small, it grows so slowly with k that it becomes it will be < 18 even when k is on the same order of magnitude as the number of particles in the observable universe. This means that, for all practical purposes, the method behaves asymptotically as a slightly slower $O(k \log_2(k))$ method, which means the speedup relative to the naive method becomes more pronounced as k becomes large.

The basic motivation of the approach—*i.e.*, the idea of approximating the Chebyshev norm with the largest p^* -norm that can be computed accurately, and then convolving according to this norm using FFT—also suggests further possible avenues of research. For instance, it may be possible to compute a single FFT (rather than an FFT at each of several contours) on a more precise implementation of complex numbers. Such an implementation of complex values could store not only the real and imaginary components, but also other much smaller real and imaginary components that have been accumulated through $+$ operations, even those which have small enough magnitudes that they are dwarfed by other summands. With such an approach would be possible to numerically approximate the max-convolution result in the same overall runtime as long as only a bounded “history” of such summands was recorded (*i.e.*, as long as only the 7 or $\log_2(\log_{1+\tau^{\frac{1}{4}}}(k))$ highest-magnitude summands was stored). In a similar vein, it would be interesting to investigate the utility of complex values that use rational numbers (rather than fixed-precision floating point values), which will be highly precise, but will increase in precision (and therefore, computational complexity of each arithmetic operation) as the dynamic range between the smallest and largest nonzero values in L and R increases (because taking L' to a large power p^* may produce a very small value). Other simpler improvements could include optimizing the error vs. runtime trade-off between the log-base of the contour search: the method currently searches $\log_2(p_{\max}^*)$ contours, but a smaller or larger log-base could be used in order to optimize the trade-off between error and runtime.

4.1 Multidimensional numerical max-convolution

The fast numerical piecewise method for max-convolution (and the affine piecewise modification) are both applicable to matrices as well as vectors (and, most generally, to tensors of any dimension). This is because the p^* -norm (as well as the derived error bounds as an approximation of the Chebyshev norm) can likewise approximate the maximum element in the tensor $u^{(m_1, m_2, \dots)}$ generated to find the max-convolution result at index m_1, m_2, \dots of a multidimensional problem, because the sum

$$\sum_{i_1, i_2, \dots} \left(u_{i_1, i_2, \dots}^{(m_1, m_2, \dots)} \right)^{p^*}$$

computed by convolution corresponds to the Frobenius norm (*i.e.* the “entry-wise norm”) of the tensor, and after taking the result of the sum to the power $\frac{1}{p^*}$, will converge to the maximum value in the tensor (if p^* is large enough).

This means that the fast numerical approx, including the affine piecewise modification, can be used without modification by invoking standard multidimensional convolution (*i.e.*, $*$). Matrix (and, in general, tensor) convolution is likewise possible for any dimension via the row-column algorithm, which transforms the FFT of a matrix into sequential FFTs on each row and column. The accompanying `python` code demonstrates the fast numerical max-convolution method on matrices, and the code can be run on tensors of any dimension (without requiring any modification).

The speedup of FFT tensor convolution (relative to naive convolution) becomes considerably higher as the dimension of the tensors increases; for this reason, the speedup of fast numerical max-convolution becomes even more pronounced as the dimension increases. For a tensor of dimension d and width k (*i.e.*, where the index bounds of every dimension are $\in \{0, 1, \dots, k-1\}$), the cost of naive max-convolution will be in $O(k^{2d})$, whereas the cost of numerical max-convolution is $O(k^d \log_2(k))$ (ignoring the $\log_2(\log_{1+\tau^{\frac{1}{4}}}(k)) \leq 18$ multiplier), meaning that there is an $O(\frac{k^d}{d \log_2(k)})$ speedup from the numerical approach. Examples of such tensor problems include graph theory, where adjacency matrix representation can be used to describe respective distances between nodes in a network.

As a concrete example, the demonstration `python` code computes the max-convolution between two 128×128 matrices. The naive method required 27.96 seconds, but the numerical result was computed in 0.589 seconds. Note that in using the error bound for tensors, any instance of k in the error bound equations should be replaced by the total number of elements in the tensor argument L (assuming L and R have similar size).

Multidimensional max-convolution can likewise be applied to hidden Markov models with additive transitions over multidimensional variables (*e.g.*, allowing the latent variable to be a two-dimensional joint distribution of American and German unemployment with a two-dimensional joint transition probability).

4.2 Max-deconvolution

The same p^* -norm approximation can also be applied to the problem of max-deconvolution (*i.e.*, solving $M = L *_{\max} R$ for R when given M and L). This can be accomplished by computing the ratio of $FFT(M^{p^*})$ to $FFT(L^{p^*})$ (assuming L has already been properly zero-padded), and then computing the inverse FFT of the result to approximate R^{p^*} ; however, it should be noted that deconvolution methods are typically less stable than the corresponding convolution methods, computing a ratio is less stable than computing a product (particularly when the denominator is close to zero).

4.3 Amortized argument for low MSE of the affine piecewise method

Although the largest absolute error of the affine piecewise method is the same as the largest absolute error of the original piecewise method, the mean squared error (MSE) of the affine piecewise method will be lower than the square of the worst-case absolute error.

To achieve the worst-case absolute error for a given contour the affine correction must be negligible; therefore, there must be two nearly vertical points on the scatter plot of $\|u^{(m_1)}\|_\infty$ vs. $\|u^{(m_1)}\|_{p^*}$, which are both extremes of the bounding envelope from **figure 3**. Thus, there must exist two different indices m_1 and m_2 with vectors where $\|u^{(m_1)}\|_{p^*} \approx \|u^{(m_1)}\|_\infty$ and where

$$\|u^{(m_2)}\|_{p^*} \approx \|u^{(m_2)}\|_\infty k_{m_2}^{\frac{1}{p^*}}$$

(creating two vertical points on the scatter plot, and forcing that both cannot simultaneously be corrected by a single affine mapping). In order to do this, it is required to have $u^{(m_1)}$ filled with a single nonzero value and for the remaining elements of $u^{(m_1)}$ to equal zero. Conversely, $u^{(m_2)}$ must be filled entirely with large, nonzero values (the largest values possible that would still use the same contour p^*). Together, these two arguments place strong constraints on the vectors L' and R' (and transitively, also constrains the unscaled vectors L and R): On one hand, filling $u^{(m_1)}$ with $k_{m_1} - 1$ zeros requires that $k_{m_1} - 1$ elements from either L or R must be zero (because at least one factor must be zero to achieve a product of zero). On the other hand, filling $u^{(m_2)}$ with all large-value nonzeros requires that k_{m_2} elements of *both* L and R are nonzero. Together, these requirements stipulate that both $k_{m_1} - 1 + k_{m_2} \leq k$, because entries of L and R cannot simultaneously be zero and nonzero. Therefore, in order to have many such vertical points, constrains the lengths of the $u^{(m_1)}, u^{(m_2)}, u^{(m_3)}, \dots$ vectors corresponding to those points. While the worst-case absolute error bound presumes that an individual vector $u^{(m)}$ may have length k , this will not be possible for many vectors corresponding to vertical points on the scatter plot. For this reason, the MSE will be significantly lower than the square of the worst-case absolute error, because making a high affine-corrected absolute error on one index necessitates that the absolute errors at another index cannot be the worst-case absolute error (if the sizes of L and R are fixed).

5 Availability

Code for exact max-convolution and the fast numerical method (both of which can be used on `numpy` arrays of any dimension, *i.e.* tensors) is implemented in `python` and available at <https://bitbucket.org/orserang/fast-numerical-max-convolution>.

Acknowledgments

We would like to thank Mattias Frånberg, Knut Reinert, and Oliver Kohlbacher for the interesting discussions and suggestions.

References

- [1] M. Boyer, G. Dufour, and L. Santinelli. Continuity for network calculus. In *Proceedings of the 21st International conference on Real-Time Networks and Systems - RTNS '13*, page 235, New York, New York, USA, October 2013. ACM Press.
- [2] D. Bremner, T. M. Chan, E. D. Demaine, J. Erickson, F. Hurtado, J. Iacono, S. Langerman, M. Patrascu, and P. Taslakian. Necklaces, Convolutions, and X+Y. December 2012.
- [3] M. Bussieck, H. Hassler, G. J. Woeginger, and U. T. Zimmermann. Fast algorithms for the maximum convolution problem. *Operations Research Letters*, 15(3):133–141, April 1994.
- [4] A. S. Eddington. *Mathematical Theory of Relativity*. Cambridge University Press, London, 1923.
- [5] G. X. Ritter and J. N. Wilson. Handbook of Computer Vision Algorithms in Image Algebra. August 2000.
- [6] O. Serang. The probabilistic convolution tree: efficient exact Bayesian inference for faster LC-MS/MS protein inference. *PLOS ONE*, 9(3):e91507, January 2014.
- [7] O. Serang. A fast numerical method for max-convolution and the application to efficient max-product inference in bayesian networks. *Journal of Computational Biology*, 2015 *in press*.
- [8] O. Serang, M. J. MacCoss, and W. S. Noble. Efficient marginalization to compute protein posterior probabilities from shotgun mass spectrometry data. *Journal of proteome research*, 9(10):5346–57, October 2010.
- [9] N. Sun and Z. Yang. The Max-Convolution Approach to Equilibrium Analysis. Technical report, December 2002.
- [10] C. Zach, D. Gallup, and J.-M. Frahm. Fast gain-adaptive KLT tracking on the GPU. In *2008 IEEE Computer Society Conference on Computer Vision and Pattern Recognition Workshops*, pages 1–7. IEEE, June 2008.